Supplementary Figures

Title: Modularity speeds up motor learning by overcoming mechanical bias in musculoskeletal geometry

Shota Hagio[1, 2] and Motoki Kouzaki[3]

[1]Graduate School of Education, The University of Tokyo, Tokyo, Japan

[2]Research Fellow of the Japan Society for the Promotion of Science, Tokyo, Japan

[3]Laboratory of Neurophysiology, Graduate School of Human and Environmental Studies, Kyoto University, Kyoto, Japan

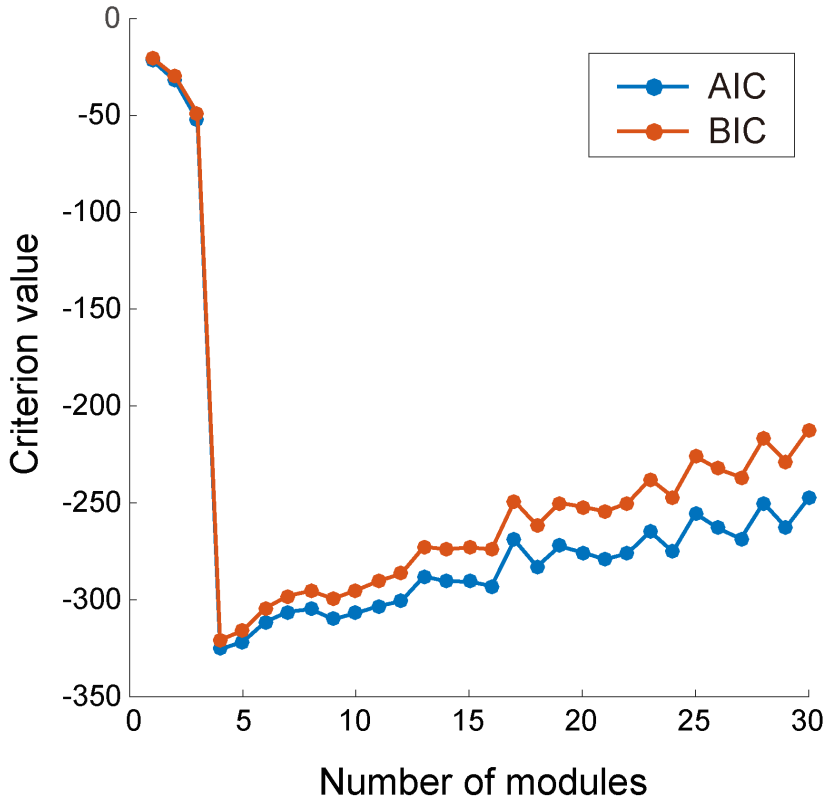

Supplementary Figure 1: Goodness of fit between model and desired toques depending on different numbers of modules in a neural network model

Goodness of fit between model and desired toques were assessed across each of 1 to 30 numbers of modules according to Akaike's information criterion (AIC) and Bayesian information criterion (BIC). The model based on 4 modules that the values of both AIC and BIC were lowest was selected.

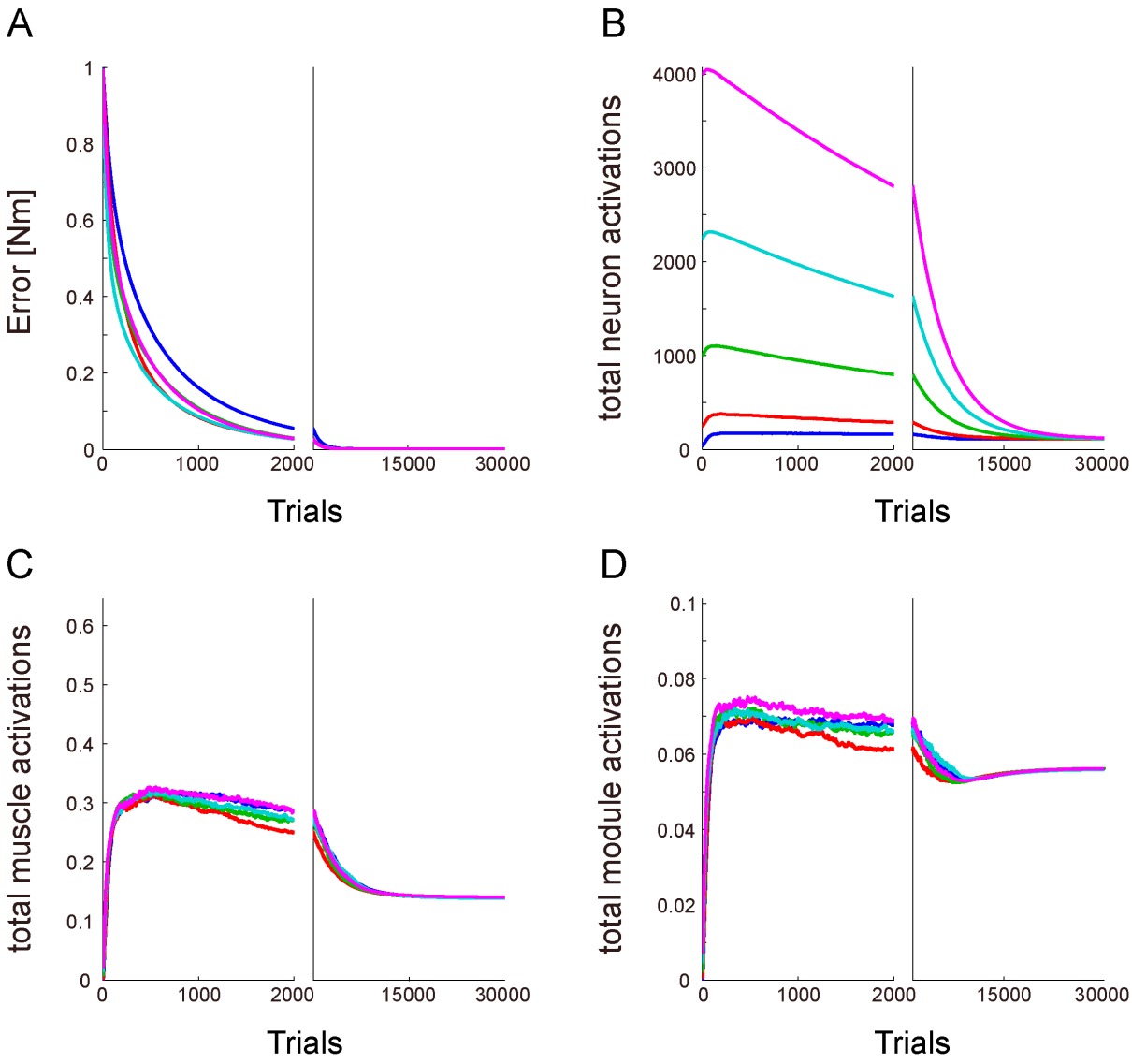

Supplementary Figure 2: Change of the network across each trial.

A: the total error between an input and output torques across trials. The modular model based on 4 modules was used. The error was gradually decreased and finally converged to zero. B-D: the total activation of neurons, modules and muscles across tasks. The origin of the right plot across each series of plots corresponds to the end of the left plot. The coloured lines represent the 5 different initial weighting matrices of M1 neurons, which were generated using the standard deviation (σ_{neu}): $\sigma_{neu} =$ 0.5 (blue), 1.0 (red), 1.5 (green), 2.0 (cyan) and 2.5 (magenta). The network state after training (t = 30,000; t: the number of trial) was robust across initial synaptic weights of neurons. There was no significant difference in the final value of task error (A) and sum of squared activations in M1 neurons (B), muscles (C) and modules (D).

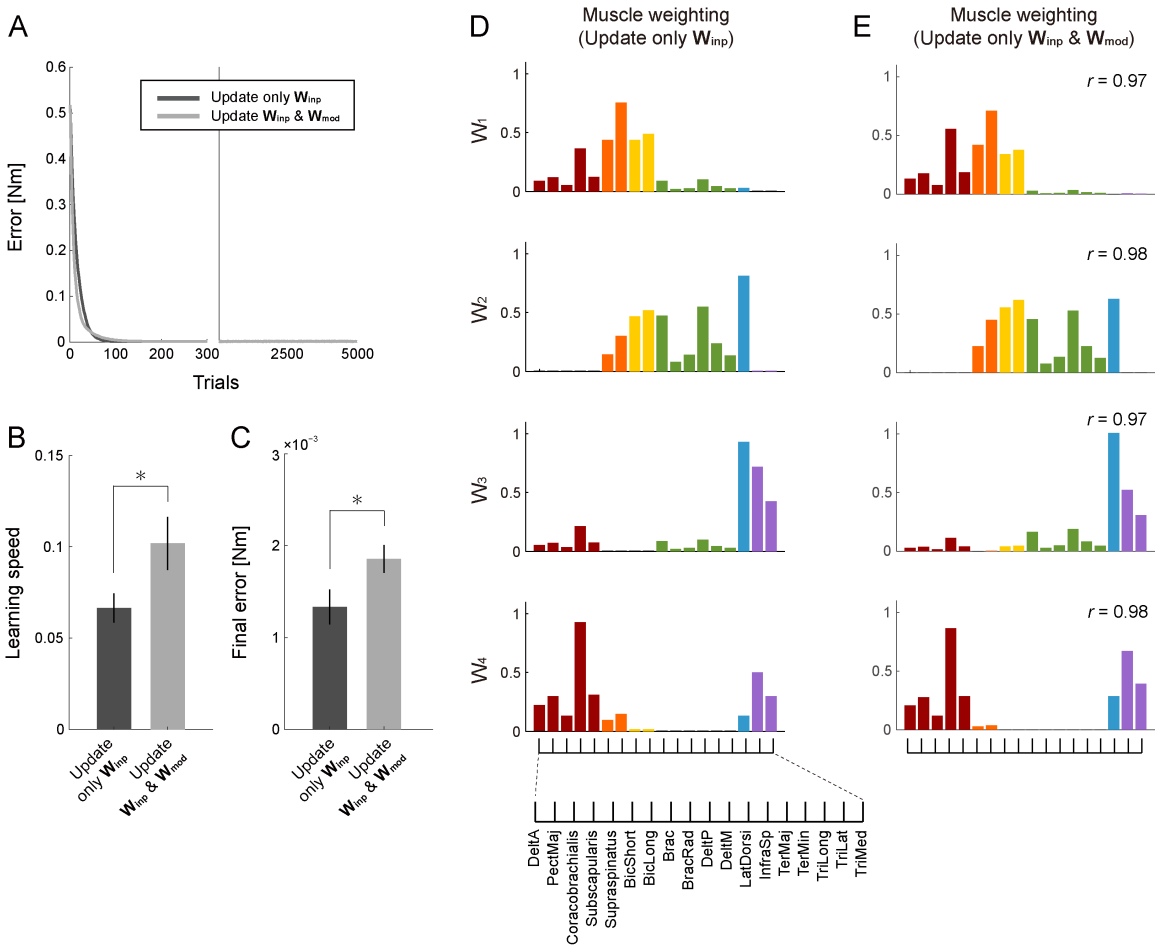

Supplementary Figure 3: Learning performance of models with updated weights to different layers

A: total error between input torques and output torques across each trial in modular models that the synaptic weights of modules, $\boldsymbol{W_{mod}}$, were updated (gray) or not (black) in addition to $\boldsymbol{W_{inp}}$. The modular model was based on 4 modules. B: averaged learning speed for 30 sets of iterations in the model that $\boldsymbol{W_{mod}}$ were updated (gray) or not (black) in addition to $\boldsymbol{W_{inp}}$. Error bars denote the standard deviation. *$p < 0.001$. C and D: muscle-weighting vectors across modules ($\mathbf{W}_{1\text{-}4}$) in the models that $\boldsymbol{W_{mod}}$ were updated or not in addition to $\boldsymbol{W_{inp}}$. The coloured bars represent mono-articular shoulder flexors (brown), bi-articular flexors (orange), mono-articular elbow flexors (yellow), mono-articular shoulder extensors (dark green), bi-articular extensor (blue-green) and mono-articular elbow extensors (purple). Muscle names are indicated by the following abbreviations: DeltA, deltoid anterior; PectMaj, pectoralis major; BicShort, biceps brachii short head; BicLong, biceps brachii long head; Brac, brachialis; BracRad, brachioradialis; DeltP, deltoid posterior; DeltM, deltoid middle; LatDorsi, latissimus dorsi; InfraSp, infraspinatus, TerMaj, teres major; TerMin, teres minor; TriLong, triceps brachii long head; TriLat, triceps brachii lateral head; TriMed, triceps brachii medial head. *r*-value denotes cosine similarity between adjacent weights.

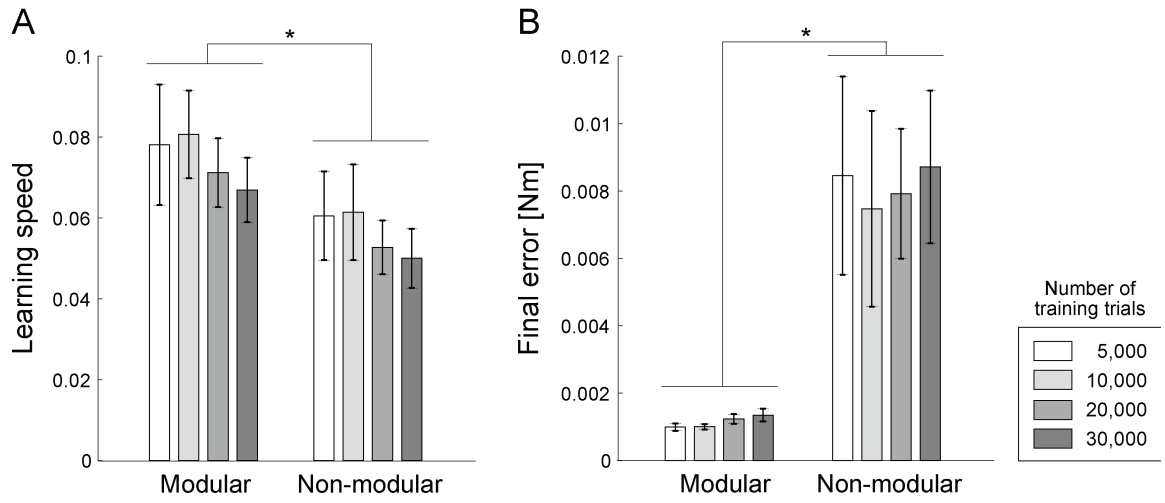

Supplementary Figure 4: Learning performance during adaptation across different state of a neural network model depending on the number of training trials.

A: averaged learning speed during adaptation to rotational perturbation across different state of a neural network model depending on the number of initial training trials, i.e., 5,000, 10,000, 20,000, and 30,000, for 30 iterations. Error bars denote the standard deviation. B: averaged total error at the end of the rotational period across the different number of training trials for 30 iterations. The modular model based on 4 modules was used. *$p < 0.001$.

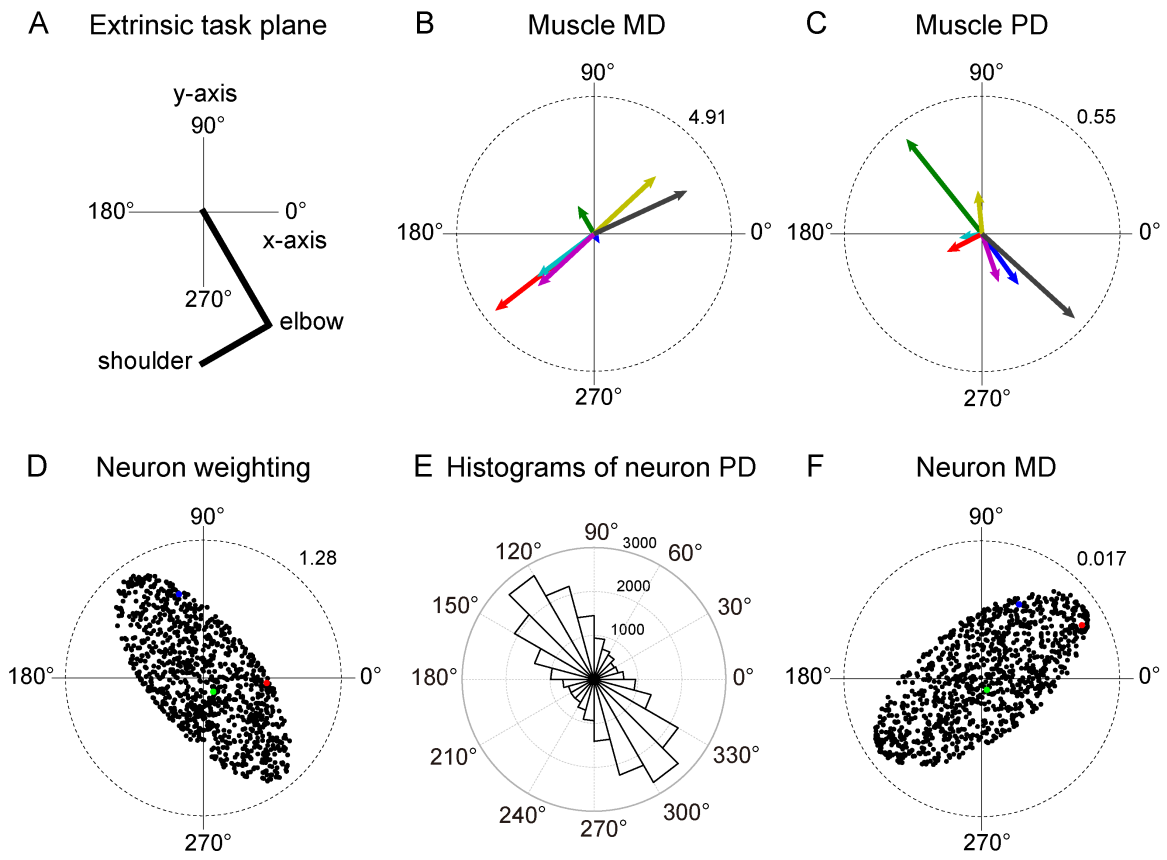

Supplementary Figure 5: Network state of neurons and muscles in 2-dimensional extrinsic tasks.

A: definition of xy coordinate in a 2-dimensional extrinsic task plane. X-axis and y-axis correspond right (positive)/left directions, and forward (positive)/backward directions on a horizontal plane, respectively. B: mechanical pulling direction vectors (MDs) of the representative muscles; subscapularis (green), BicShort (cyan), BicLong (red), Brac (purple), DeltP (blue), TriLong (grey) and TriLat (yellow). C: averaged preferred directions (PDs) of the representative muscles for 30 sets of iterations. The colours correspond to those in B. D: synaptic weights of each M1 neuron are shown as dots on the xy coordinate. The weightings were bimodally distributed. E: polar histograms of the PD of neurons for 30 sets of iterations. F: MD of M1 neurons on the xy coordinate. The neuron MDs were distributed bimodally and approximately perpendicular to the bimodal axis of neuron weightings. The coloured dots (blue, red and green) in D and F represent the same neurons. The direction in the polar coordinates corresponds to those in A. The modular model based on 4 modules was used.

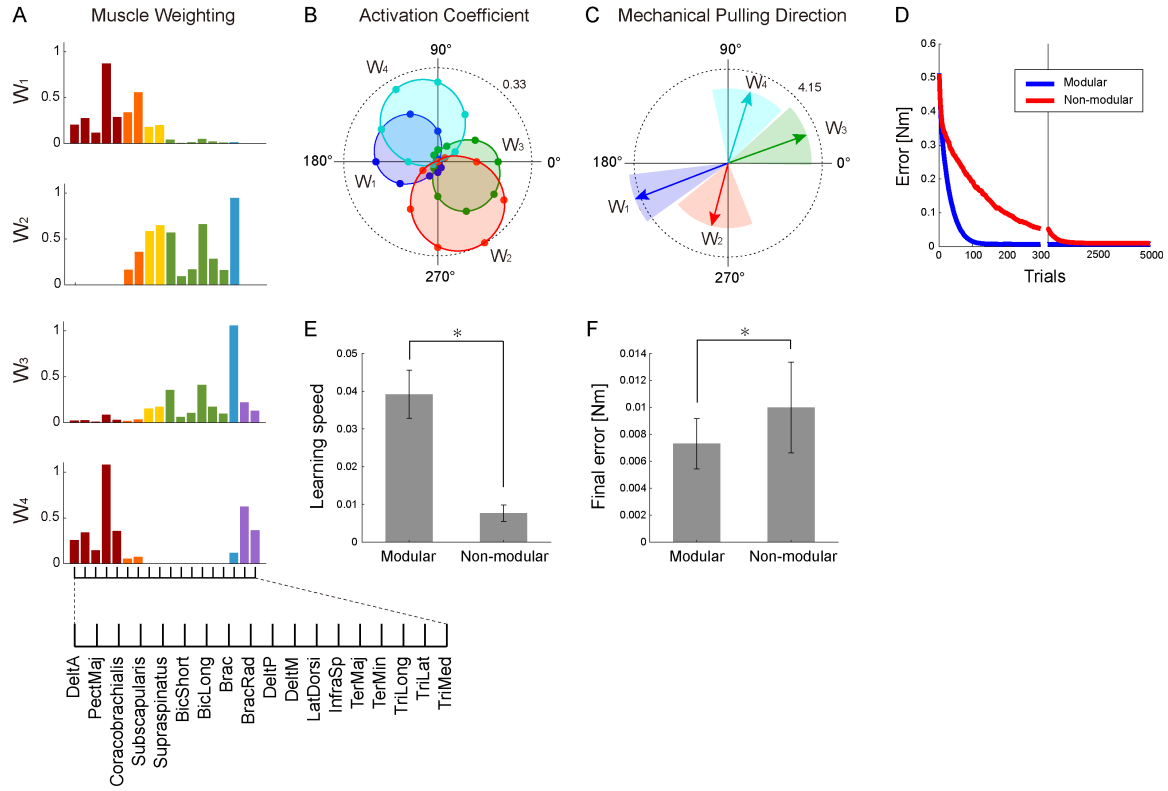

Supplementary Figure 6: Network state of modules and learning performance in the rotational period.

A: muscle-weighting vectors across modules ($\mathbf{W}_{1\text{-}4}$). The coloured bars represent mono-articular shoulder flexors (brown), bi-articular flexors (orange), mono-articular elbow flexors (yellow), mono-articular shoulder extensors (dark green), bi-articular extensor (blue-green) and mono-articular elbow extensors (purple). B: averaged activation coefficient of each module on the xy coordinate for 30 sets of iterations. C: averaged MD of each module on the xy coordinate for 30 sets of iterations. The coloured shading represents the standard deviation of the angle of MD across each iteration. The direction in the polar coordinates corresponds to those in Supplementary Fig. 4A. D: total error between input and output fingertip accelerations across each trial in the model with (blue) and without (red) modules. E: averaged learning speed for 30 sets of iterations in the model with and without modules. Error bars denote the standard deviation. F: averaged total task error at the end of the rotational period for 30 sets of iterations in the model with and without modules. *p < 0.001.

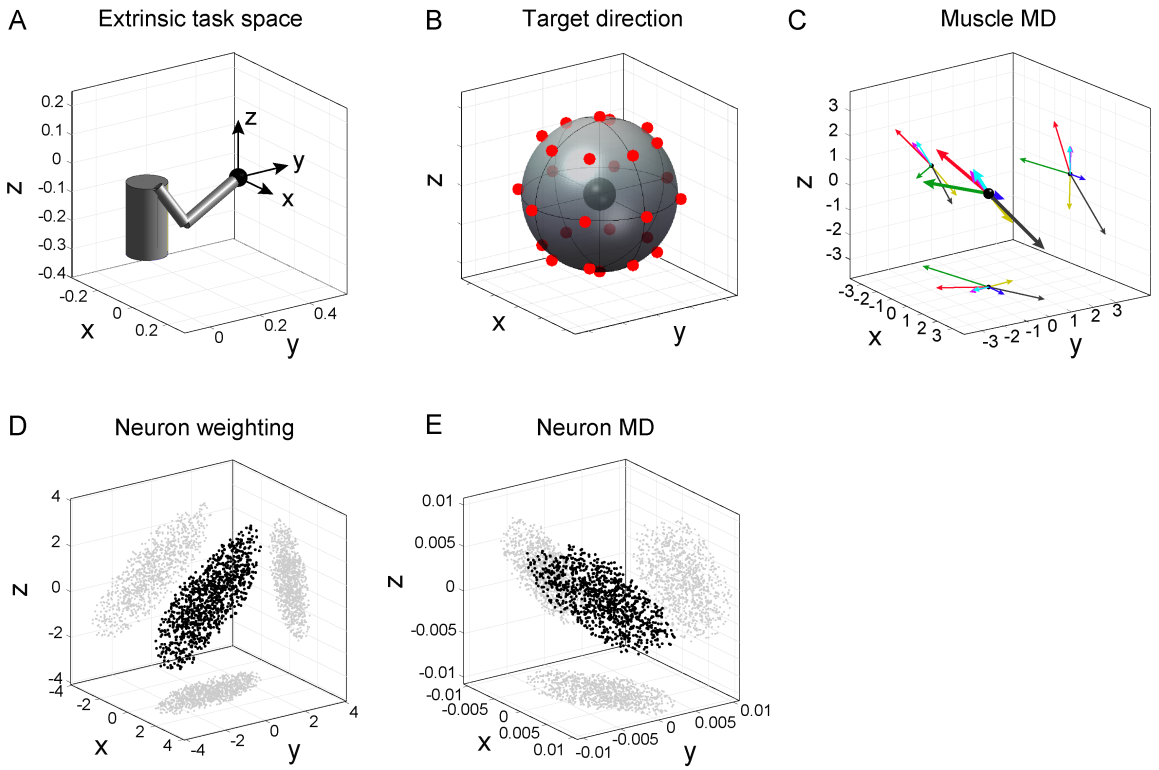

Supplementary Figure 7: Network state of neurons and muscles in 3-dimensional extrinsic tasks.

A: definition of xyz coordinate in 3-dimensional extrinsic task space. X-axis, y-axis and z-axis correspond right (positive)/left directions, forward (positive)/backward directions, and upward (positive)/downward directions, respectively. B: 33 target directions for producing fingertip acceleration were distributed on the surface of sphere in the 3-dimensional extrinsic space. The amplitudes of the fingertip acceleration were equal, which was set to 1 m/s^2. C: mechanical pulling direction vectors (MDs) of the representative muscles; subscapularis (green), BicShort (cyan), BicLong (red), Brac (purple), DeltP (blue), TriLong (grey) and TriLat (yellow). Graph walls display a 2-dimensional projection of the muscle MDs. D: synaptic weights of each M1 neuron are shown as dots in the xyz coordinate. Graph walls display a 2-dimensional projection of the neuron weightings. E: MD of M1 neurons in the xyz coordinate. Graph walls display a 2-dimensional projection of the neuron MDs. The direction in the xyz coordinates corresponds to those in A. The modular model based on 6 modules was used.

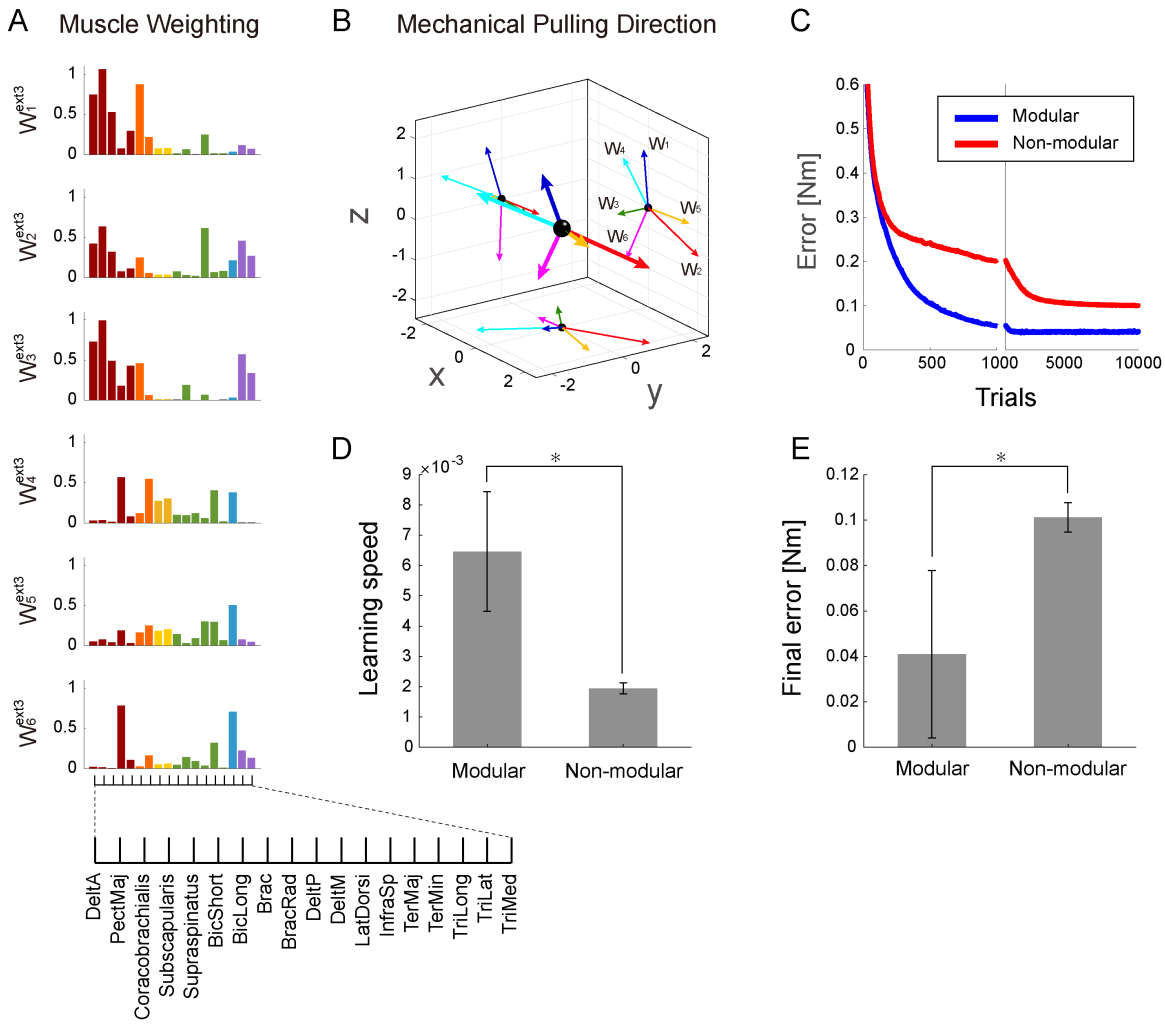

Supplementary Figure 8: Network state of modules and learning performance in the rotational period.

A: muscle-weighting vectors across modules ($\mathbf{W}_{1-6}^{ext3}$). The coloured bars represent mono-articular shoulder flexors (brown), bi-articular flexors (orange), mono-articular elbow flexors (yellow), mono-articular shoulder extensors (dark green), bi-articular extensor (blue-green) and mono-articular elbow extensors (purple). B averaged MD of each module on the xyz coordinate for 30 sets of iterations. The representation of $\mathbf{W}_{1\text{-}6}$ was corresponding to $\mathbf{W}_{1-6}^{ext3}$ in A. Graph walls display a 2-dimensional projection of the module MDs. The direction in the xyz coordinate corresponds to those in Supplementary Fig. 6A. C: total error between input and output fingertip accelerations across each trial in the model with (blue) and without (red) modules. D: averaged learning speed for 30 sets of iterations in the model with and without modules. Error bars denote the standard deviation. E: averaged total task error at the end of the rotational period for 30 sets of iterations in the model with and without modules. *$p < 0.001$.

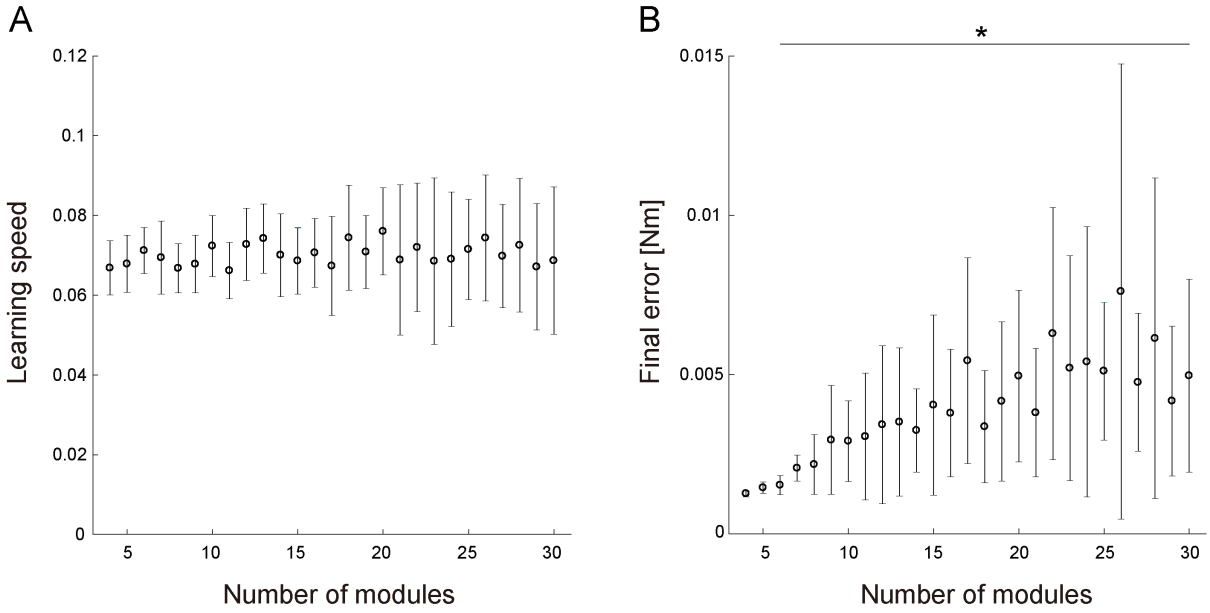

Supplementary Figure 9: Learning performance across the number of modules.
A: averaged learning speed across 4 to 30 modules for 30 iterations. Error bars denote the standard deviation. B: averaged total error at the end of the rotational period across 4 to 30 modules for 30 iterations. Asterisks represent the significant difference from the 4 modules. Asterisk denotes significant difference with the value in the model with 4 modules ($p < 0.05$).